



Paleomagnetic dating: Methods, MATLAB software, example



Danny Hnatyshin^{a,*}, Vadim A. Kravchinsky^b

^a Department of Earth and Atmospheric Sciences, University of Alberta, Edmonton, Alberta T6G 2E1, Canada

^b Department of Physics, University of Alberta, Edmonton, Alberta T6G 2E1, Canada

ARTICLE INFO

Article history:

Received 7 March 2014

Received in revised form 4 May 2014

Accepted 9 May 2014

Available online 17 May 2014

Keywords:

Age dating software

Geological dating

Gold mineralization

Ore deposit formation

Paleomagnetism

Plotting software

ABSTRACT

A MATLAB software tool has been developed to provide an easy to use graphical interface for the plotting and interpretation of paleomagnetic data. The tool takes either paleomagnetic directions or paleopoles and compares them to a user defined apparent polar wander path or secular variation curve to determine the age of a paleomagnetic sample. Ages can be determined in two ways, either by translating the data onto the reference curve, or by rotating it about a set location (e.g. sampling location). The results are then compiled in data tables which can be exported as an excel file. This data can also be plotted using variety of built-in stereographic projections, which can then be exported as an image file. This software was used to date the giant Sukhoi Log gold deposit in Russia. Sukhoi Log has undergone a complicated history of faulting, folding, metamorphism, and is the vicinity of many granitic bodies. Paleomagnetic analysis of Sukhoi Log allowed for the timing of large scale thermal or chemical events to be determined. Paleomagnetic analysis from gold mineralized black shales was used to define the natural remanent magnetization recorded at Sukhoi Log. The obtained paleomagnetic direction from thermal demagnetization produced a paleopole at 61.3°N, 155.9°E, with the semi-major axis and semi-minor axis of the 95% confidence ellipse being 16.6° and 15.9° respectively. This paleopole is compared to the Siberian apparent polar wander path (APWP) by translating the paleopole to the nearest location on the APWP. This produced an age of 255.2 ± 31.0 Ma and is the youngest well defined age known for Sukhoi Log. We propose that this is the last major stage of activity at Sukhoi Log, and likely had a role in determining the present day state of mineralization seen at the deposit.

© 2014 Elsevier B.V. All rights reserved.

1. Introduction

Paleomagnetism is the study of how the Earth's magnetic field is recorded in ancient materials such as rocks and sediments. Since magnetic minerals (e.g. magnetite, hematite) are almost ubiquitous in rocks and sediments, paleomagnetic studies can be applied to a wide range of substances. These magnetic grains will attempt to align themselves with the local magnetic field until they become locked into place. This is known as remanent magnetization, and can be described by its inclination, declination, and intensity, or by the related values of paleolatitude and paleolongitude which are used to define a paleopole.

When a sequence of paleopoles is well defined in age they can be plotted together in order to produce what is known as an apparent polar wander path (APWP). This path is constructed using known paleopoles for a stable continental block which represents the apparent wander of paleopoles through time for that continent. Ultimately this can be used as a reference for other paleopoles gathered for that continental block. For paleomagnetic dating the APWP is used to date a pole obtained from rocks or sediments of undefined age by linking the

paleopole to the nearest point on the APWP (Blanco et al., 2013; Kravchinsky and Kabin, 2005).

A similar idea arises with secular variation, the cycle of rotation around the Earth's rotational axis that a magnetic pole undergoes over thousands of years. Similar to an APWP, these secular variation (SV) curves typically are used to display inclination, declination, and the intensity of the magnetic field for a given region through time. The SV curves are typically defined for only the last few thousand years, which is useful when dating young material such as archeological artifacts (Hagstrum and Blinman, 2010; Pavon-Carrasco et al., 2011; Tanguy et al., 2003).

Recently there has been great strides in creating well defined techniques and useful computer software to date archeological artifacts (archeomagnetism) using inclination, declinations, and intensities (Le Goff et al., 2002; Pavon-Carrasco et al., 2011). Paleomagnetic dating, a study mostly concerned with sediments, rocks, and tectonic processes, has also been used with success in the past (Blanco et al., 2013; Symons and Arne, 2005; Symons and Sangster, 1991). However, there is often a lack of communication into the exact method used in dating the geologic material via paleomagnetism. The primary goal of this paper is to provide the community with a software package that can take paleomagnetic data from undated material (rocks, sediments, artifacts) and compare them with a user defined reference curve (APWP or SV).

* Corresponding author. Tel.: +1 780 4925591; fax: +1 780 4920714.
E-mail address: dh10@ualberta.ca (D. Hnatyshin).

The giant Sukhoi Log gold deposit in Russia will act as a case study for this project as this area is in need of additional age constraints to help pin down the timing of the complex metamorphic and mineralization history of this deposit. Any additional constraints based on our remanent magnetization age will help piece together the history of this important gold deposit.

2. Geologic setting and mineralization

Sukhoi Log is a large, low to moderate grade gold and platinum-group element (PGE) deposit found in the Lena gold bearing district of Siberia (58.7°N, 115.2°E) (Fig. 1). The deposit is hosted within a complicated regional structure known as the Badaibo synclinorium that has gone through many stages of faulting, folding, and metamorphism. The synclinorium has undergone green schist metamorphism, and is the vicinity of a number of Palaeozoic (~270–340 Ma) granitic intrusions (Tsygankov et al., 2007; Wood and Popov, 2006). An igneous body is also assumed to exist directly underneath Sukhoi Log itself based on geophysical evidence (Distler et al., 2004). The majority of the mineralization is contained within black shales of the Khomolkho Formation inside an overturned anticline (Distler et al., 2004; Wood and Popov, 2006).

The most economically important type of mineralization is the gold mineralization that occurs in the core of the anticline, however there has been renewed interest into PGE mineralization found on the periphery of the deposit (Distler et al., 2004). Gold mineralization is primarily

associated with disseminated pyrite and bedding parallel pyrite–quartz veins (Distler et al., 2004; Large et al., 2007; Meffre et al., 2008). The gold is typically found in pyrite at the ppm level or as native gold inclusions within the sulfide minerals of the ore deposit (Distler et al., 2004; Large et al., 2007, 2009; Meffre et al., 2008). Platinum is generally found as either a native metal or an alloy on the outskirts of the gold mineralization (Distler et al., 2004).

3. Previous age constraints

The region has undergone very complex tectonic and magmatic activity which has complicated the interpretation of the deposit. The longstanding question is when did the gold get introduced to the system, and if it has been modified, through either metamorphism or the hydrothermal activity associated with magmatism.

The upper bound age of the deposit is constrained by the age of the host rock, while granite and metamorphic ages provide information on the timing of other major geologic events in the region. Studies by Meffre et al. (2008) and Yudovskaya et al. (2011) attempted to estimate the host rock age and metamorphic history of Sukhoi Log by dating zircon and monazite using U–Pb and U–Th–Pb methods. The youngest detrital zircons analyzed by Meffre et al. (2008) have a U–Pb age of 600 ± 10 Ma which can be considered as an upper bound age of the host rocks. The monazite samples that Meffre et al. (2008) analyzed also give an estimate of the metamorphic history of the region. Monazite cores were dated to 573 ± 12 Ma, while the rims correspond to an age of 516 Ma,

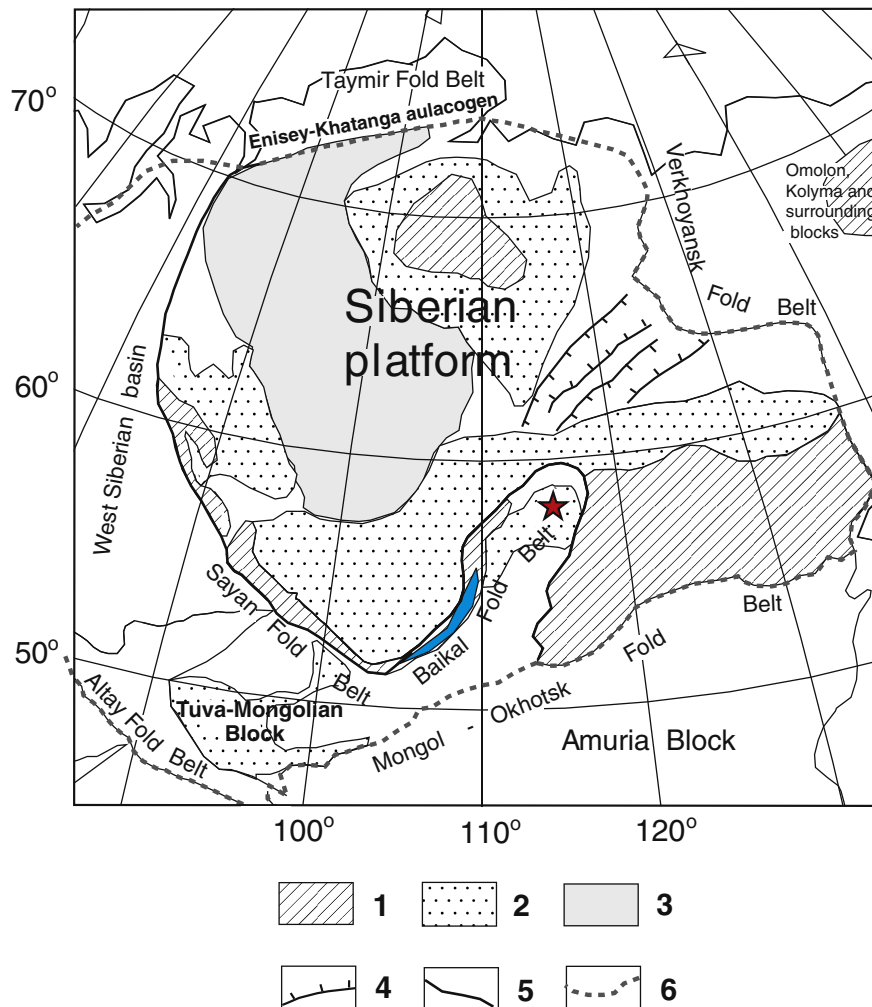


Fig. 1. Simplified geological structure of Siberia and surrounding regions (modified from Kravchinsky et al., 2002). 1 – Precambrian shields; 2 – Riphean and Paleozoic sediment cover; 3 – Permian–Triassic traps; 4 – Viluy paleorift; 5 – edge of Precambrian platform; 6 – Middle–Late Paleozoic border of Siberian block.

which gives the broad timeline of metamorphism in the area, and is similar to previous estimates of metamorphism reported by Distler et al. (2004).

A subsequent study by Yudovskaya et al. (2011) disputes these young ages for host rock deposition and metamorphism based on their analysis of zircon and monazite. Metamorphic monazite ages reported by Yudovskaya et al. (2011) were substantially higher than that of Meffre et al. (2008) and peak at ~650 Ma. Yudovskaya et al. (2011) argued that the detrital zircons measured in the earlier study of Meffre et al. (2008) must actually be the age of growth or rejuvenation of these zircons during metamorphism, and therefore are not true detrital zircons. Combining the monazite data with detrital zircon data Yudovskaya et al. (2011) argued for host rock formation occurring at ~800 Ma and the subsequent metamorphism occurring at 570–650 Ma.

Other, much younger ages have also been reported at Sukhoi Log. Hydrothermal monazite ages from the Yudovskaya et al. (2011) study have been measured to be 440–450 Ma in age, which is similar to the 447 ± 7 Ma date obtained for a whole rock Rb–Sr isochron by Laverov et al. (2007). The youngest ages reported at Sukhoi Log include monazite ages of 374 ± 20 Ma and 288 ± 22 Ma from Meffre et al. (2008), and a quartz vein Rb–Sr age of 321 ± 14 Ma from Laverov et al. (2007). These youngest ages tend to be similar to the ages of a number nearby Palaeozoic granites (Kuz'min et al., 2006; Larin et al., 1997; Tsygankov et al., 2007). These ages have been used to suggest that Palaeozoic technomagmatic activation introduced gold to Sukhoi Log at either ~450 Ma (Yudovskaya et al., 2011) or ~320 Ma (Laverov et al., 2007). Kuzmin et al. (2010) suggested that such activation was triggered by the early stage of the Siberian trap large igneous province formation.

Studies on the complex paragenesis of the sulfides at Sukhoi Log help provide other constraints on the timing of gold mineralization (Large et al., 2007, 2009; Meffre et al., 2008). Large et al. (2007, 2009) identified five distinct pyrite types at Sukhoi Log, the first two likely being of diagenetic origin, type three being formed near the beginning of metamorphism, type four being associated with peak metamorphism, and type five forming sometime after peak metamorphism. Large et al. (2009) used the distribution of trace elements within these different pyrite generations to argue that the majority of gold must be introduced during digenesis and into early metamorphism (pyrite types 1–3). The later stage pyrite did not appear to be associated with new gold influx but was associated with gold remobilization occurring during later stage hydrothermal activity at Sukhoi Log. These observations by themselves do not give the absolute age of gold introduction or remobilization but provide useful guidelines on how to interpret the dates provided in other studies.

4. Paleomagnetic methods

We have sampled 7 sites separated by 20–200 m in the Sukhoi Log main adit with gold mineralization among black shales with various beddings. We applied the magnetic azimuth corrections to the bedding and the sample orientation. Generally two 8 cm³ cubes (referred to as samples) were cut from each oriented hand block. We obtained the results from 50 samples with 47 samples representing different hand blocks. Stepwise thermal demagnetization and magnetic measurements of the samples were carried out at the Physics Department of the University of Alberta. The first attempt to study Sukhoi Log gold mineralization zone was performed by Zhitkov and Kravchinsky in 1982 on a few pilot samples without comprehensive component analysis and stepwise demagnetization. Their result was promising but unreliable.

The samples were thermally demagnetized in ovens housed in a permalloy magnetically shielded room. The residual field was approximately 8–12 nT in the center of the oven. The samples were demagnetized using 25 °C steps to around 600 °C, and remanent magnetizations were measured with a 3-axis 2G cryogenic magnetometer.

Magnetic susceptibility was measured using a Bartington susceptibility-meter in order to characterize mineralogical changes during the heating. Such changes took place in 60% of the samples after 400–500 °C.

The data was processed using software of Enkin (1996) and Cogné (2003) and orthogonal projections of vector behavior diagrams (Zijderveld, 1967) were constructed for each sample to aid in interpretation of the demagnetization data. Resolved components were analyzed using principal component analysis (PCA) (Kirschvink, 1980) and site-mean directions were calculated using Fisher (1953) statistics. For mixed populations of directions and remagnetization great circles, the combined analysis technique of McFadden and McElhinny (1988) was also used in the analysis. Tables in this paper include only samples with directions used for our statistical analysis.

In addition, rock magnetic measurements were completed to aid in the identification of magnetic mineralogy and changes to this mineralogy that occurred during thermal demagnetization. These measurements included temperature dependant magnetic susceptibility, using the Bartington system, and isothermal remanent magnetization (IRM) acquisition.

A high temperature magnetic susceptibility scan was performed on several samples using a Bartington MS2W system. The temperature of the samples was increased from room temperature to 700 °C and the magnetic susceptibility was measured every 2 °C. Once the samples had finished heating to 700 °C, they were allowed to cool to room temperature and the magnetic susceptibility was taken at 2 °C increments. At 270–320 °C many samples show a change in the rate of increasing magnetic susceptibility (MS) (Fig. 2A). We interpret this change as a signature of pyrrhotite which can be observed microscopically and is reported as a part of the complex sulfide paragenesis. The minimum of magnetic susceptibility is reached at approximately 590 °C. IRM acquisition experiments are dominated by saturation magnetizations between 250 and 300 mt, in the samples used for paleomagnetic measurements (Fig. 2B). We interpret these results to show that the natural remanent magnetization (NRM) is most likely carried by magnetite grains.

5. Paleomagnetic result

Demagnetization using an alternating field was not effective for isolating primary magnetization and therefore was tested only on pilot samples. A low temperature component was defined between the 20 °C and 250–400 °C on the basis of PCA analysis of the stepwise thermal demagnetization data (Fig. 3). This magnetic component often has a northerly declination and downward inclination in in-situ coordinates, and primary displays normal polarity. The component is very scattered which does not allow calculating the average direction.

The high-temperature component (HTC) was identified during thermal demagnetization steps between 300 and 600 °C (Fig. 3) and always displays steep inclinations and declinations directed to the southeast. Increasing magnetic susceptibility values at temperatures above 300–400 °C are typical of approximately 50% of the thermally demagnetized samples, and interpreted to indicate mineralogical changes occurring within the samples during demagnetization resulting from thermal oxidation. Such samples demonstrated only low temperature component and were excluded from further analysis unless great circles could be easily identified. We interpret such behavior as magnetization carried by pyrrhotite dominated samples. Samples which had blocking temperatures at 400–600 °C contained well-preserved low and high temperature components. All sampled sites contained only reverse polarity (Table 1).

The average of the high temperature component at the site level (Table 1) is $D_g = 245.1^\circ$, $I_g = -79.6^\circ$ ($k = 49$, $\alpha_{95} = 8.7^\circ$) for in-situ coordinates, and $D_s = 223.4^\circ$, $I_s = -54.4^\circ$ ($k = 18.4$, $\alpha_{95} = 14.4^\circ$) in tilt-corrected coordinates (Fig. 4). Applying of the fold test (McFadden, 1990) for the HTC gives maximum at 0% (fold test negative). Fold test of Enkin (2003) for HTC gives similar result (0% of maximum unfolding).

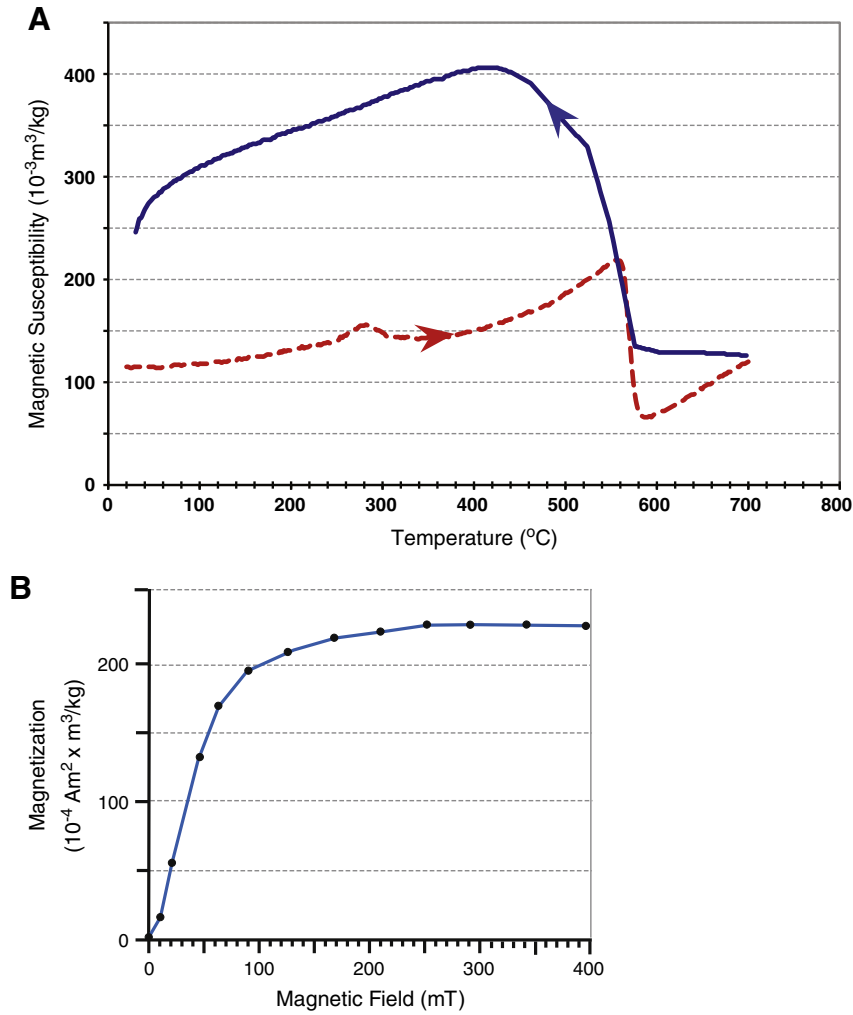


Fig. 2. Typical results of rock magnetic experiments for Sukhoi Log ore samples. A – thermal dependent magnetic susceptibility measurements. Temperature was increased from room temperature to 700 °C (red dashed line) and cooled back to room temperature (blue solid line). B – isothermal remanent magnetization (IRM) acquisition curves.

Paleomagnetic pole for the in-situ HTC is given in Table 2 and discussed further in the text.

6. Dating techniques

To determine the age of a paleopole (or archeomagnetic direction) a technique similar to that of Kravchinsky et al. (2004) and Blanco et al. (2013) was developed. Our method requires that the paleomagnetic pole obtained for a study be translated such that the paleopole intersects a chosen APWP. Choosing an appropriate APWP is a crucial aspect of this dating technique, and can be obtained from a database (for example, Torsvik et al., 2012) or can be constructed independently. Two major types of APWP are commonly encountered, a spline path which creates a smooth path through paleopoles of known age, and a running mean path that averages poles with specific time windows to create an APWP. The results of these interpolations are newly calculated poles at well defined intervals (e.g. every 10 Ma in the Torsvik et al., 2012 dataset), which can be connected to form an APWP. High resolution curves are desired so that proper intersections between the paleopole and the APWP are achieved. We apply linear interpolation between adjacent points on any inputted APWP to create an APWP based on points that are no further than 0.1° apart in either latitude or longitude. This was done to ensure that intersections between the APWP and a

paleopole are well defined. If the inputted APWP has a positional uncertainty such that there is an associated error ellipse (A_{95}) around each pole that defines the APWP, interpolation in this error is also required. To calculate the A_{95} at any point along the APWP consider the situation in Fig. 5. In Fig. 5 there are two poles, A and B, which define the APWP. Each of these poles has a different age and A_{95} . Suppose then that we want to calculate what the expected A_{95} would be at a point C between them. To find this A_{95} for point C (defined in Fig. 5 as CA_{95}) we use the following two equations:

$$\text{ang}_{i,j} = \cos^{-1} \left[\cos(\text{lat}_i) * \cos(\text{lon}_i) * \cos(\text{lat}_j) * \cos(\text{lon}_j) + \cos(\text{lat}_i) * \sin(\text{lon}_i) * \cos(\text{lat}_j) * \sin(\text{lon}_j) + \sin(\text{lat}_i) * \sin(\text{lat}_j) \right] \quad (1)$$

where ang_{ij} is the angular distance between poles i and j , lat is the latitude of the pole, and lon is the longitude of the pole.

$$CA_{95} = AA_{95} - \frac{\text{ang}_{A,C}}{\text{ang}_{A,B}} (AA_{95} - BA_{95}) \quad (2)$$

where CA_{95} is the A_{95} for intersection point C, AA_{95} is the A_{95} for point A, and BA_{95} is the A_{95} for point B. $\text{ang}_{A,C}$ is defined as the angular distance between points A and C, and $\text{ang}_{A,B}$ is defined as the angular distance

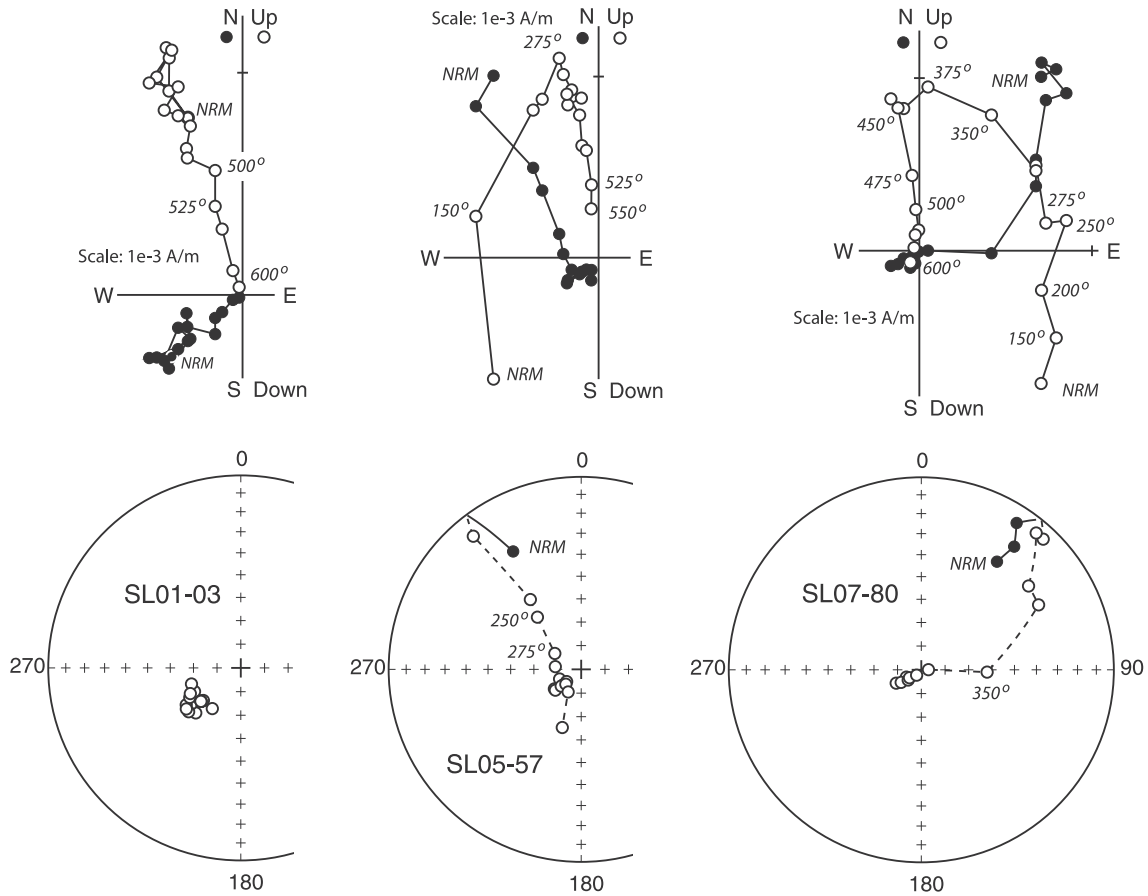


Fig. 3. Results of thermal demagnetization of Sukhoi Log samples. Top – thermal demagnetization orthogonal vector plots in-situ coordinates (Zijderveld, 1967); bottom – typical equal-area projections illustrating demagnetization paths during experiments. Closed (open) symbols in orthogonal plots: projections onto the horizontal (vertical) plane; temperature steps are indicated in degrees Celsius.

between points A and B. The A_{95} for each point along the APWP is bounded by two lines that connect poles A and B. With both A_{95} and α_{95} being known at the intersection point, they can be combined using:

$$dp' = \sqrt{(dp_{pole}^2 + CA_{95}^2)} \tag{3}$$

Table 1
Site-mean paleomagnetic directions for the high temperature component of magnetization for the Sukhoi Log gold deposit mineralization zone (58.7°N, 115.2°E).

Site	N	Dg	Ig	Ds	Is	k-Value	α_{95}	Note
SL01	7	227.4°	-77.7°	-	-	97.2	6.2°	
		-	-	224.3°	-46.3°	80	6.8°	
SL02	8	117.5°	-80.1°	168.7°	-57.8°	53.5	7.6°	
SL03	6	301.2°	-76.8°	-	-	60.7	9°	4d2cc
		-	-	230.1°	-54°	25	14.2°	4d2cc
SL04	7	248.4°	-79.1°	-	-	96	6.2°	
		-	-	170.3°	-50°	75.9	7°	
SL05	8	232°	-82.1°	-	-	416.7	2.8°	
		-	-	247.1°	-55.4°	93.2	6°	
SL06	8	266.4°	-75.2°	-	-	77.2	6.5°	6d2cc
		-	-	232.8°	-44.7°	19.3	13.1°	6d2cc
SL07	6	237.4°	-62.9°	209.9°	-49.1°	63.7	8.5°	
Overall	7	245.1°	-79.6°	-	-	49	8.7°	
Mean sites	-	-	-	213.4°	-54.4°	18.4	14.4°	

Notes: (N) number of samples or sites, which contributed directions (d) or great circles (cc) in the calculation of the site mean, coordinates of geographic (in-situ) declination and inclination (D_g, I_g) and stratigraphic declination and inclination (D_s, I_s), Fisher estimate of kappa (k-value), and the half angle radius of the 95% probability confidence cone (α_{95}).

$$dm' = \sqrt{(dm_{pole}^2 + CA_{95}^2)} \tag{4}$$

where $dp_{95'}$ and $dm_{95'}$ define the new confidence ellipse of the paleopole. The terms dp_{pole} and dm_{pole} are the original dimensions of the paleopole's confidence ellipse, and CA_{95} is the A_{95} for the APWP at the intersection point. The results of these calculations can be seen in the example provided in Fig. 6.

To date a paleopole, the ages of intersections for both the pole and confidence ellipse ($\alpha_{95'}$) need to be determined. This is done in a similar fashion to Eq. (2) where the age of the intersection point is given by the equation:

$$C_{age} = A_{age} - \frac{ang_{A,C}}{ang_{A,B}} (A_{age} - B_{age}) \tag{5}$$

where C_{age} is the age of some point located between the two APWP poles A and B. Both points A and B have associated ages A_{age} , and B_{age} respectively.

To show how this equation is applied, consider the situation presented in Fig. 7. For any confidence ellipse there will be at least three intersections with the APWP, one intersection for the paleopole itself, one for the lower bound age of the confidence ellipse, and one for the upper bound age of the confidence ellipse. For example, if we define the age of $A < B < C < D < E$ for Fig. 7, then Point 2 is defined to be the lower bound age and Point 3 is defined as upper bound age. To calculate the actual age we apply Eq. (4) three separate times, once for the paleopole (Point 1) and once for both the lower (Point 2) and upper (Point 3) bound ages. Point 4 is not considered a valid intersection

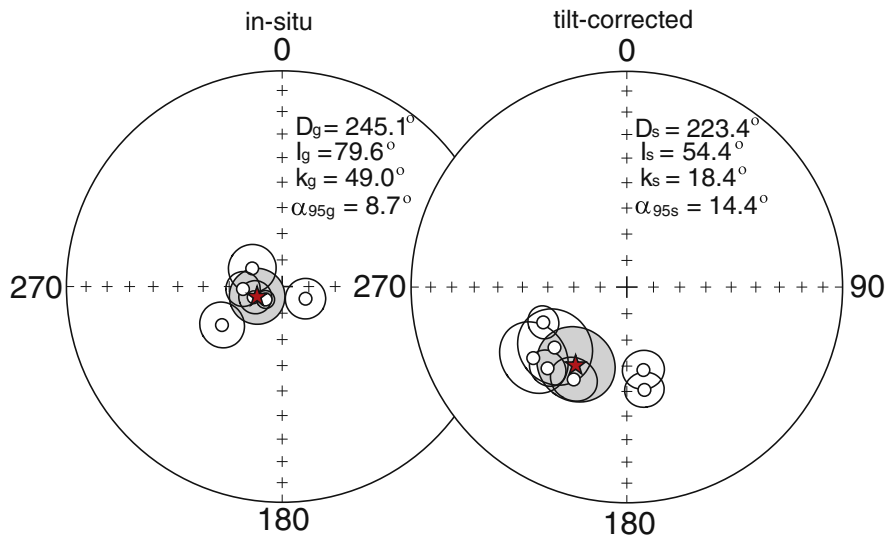


Fig. 4. Equal-area projections of site-mean directions of high-temperature (HTC) components, with circles of 95% confidence for Sukhoi Log sites in-situ (left) and tilt-corrected (right). Closed (open) symbols – downward (upward) inclinations. Star: formation mean directions.

Table 2
Paleomagnetic pole of the Sukhoi Log gold deposit mineralization zone.

Geographic coordinates	Pole latitude/pole longitude	dp/dm
58.7°N/115.2°E	61.3°/155.9°	15.9°/16.6°

Notes: pole latitude, pole longitude: latitude, longitude of the paleomagnetic pole; dp, dm: semi-axes of the 95% confidence ellipse of paleomagnetic pole.

since the APWP must leave the paleopole's confidence ellipse to reach this intersection point.

6.1. Angular method

In general a paleopole will rarely intersect a given APWP and therefore must be translated to a point on the APWP. This can be accomplished by determining the angular distance between a paleopole and every point on the APWP. Potential ages occur at points where the angular distance reaches a local minimum, and the most probable age occurs at the global minimum (Fig. 8).

6.2. Rotation method

In some situations, geologic terrains are known or are suspected to have undergone rotations as a result of a complex tectonics. In these cases a paleopole has been rotated along a small circle, centered on the site location, away from its original position. In such a case a counter

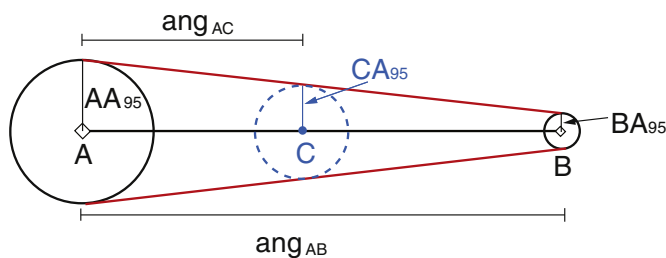


Fig. 5. Consider two paleopoles (diamonds) that define an APWP (black line connecting the diamonds) with two different A_{95} 's (AA_{95} for pole A, and BA_{95} for pole B). Point C lies between A and B and is bounded by the two solid red lines which define the A_{95} for each point along the APWP. ang_{AB} = angular distance between A and B, ang_{AC} = angular distance between A and C.

rotation must be applied to find its true age. Possible ages are calculated by dividing the small circle into a series of points that differ by no more than 1° latitude or longitude. For each point along the small circle the minimum angular distance to the APWP is determined. This results in a dataset where each point on the small circle, as defined by its rotation,

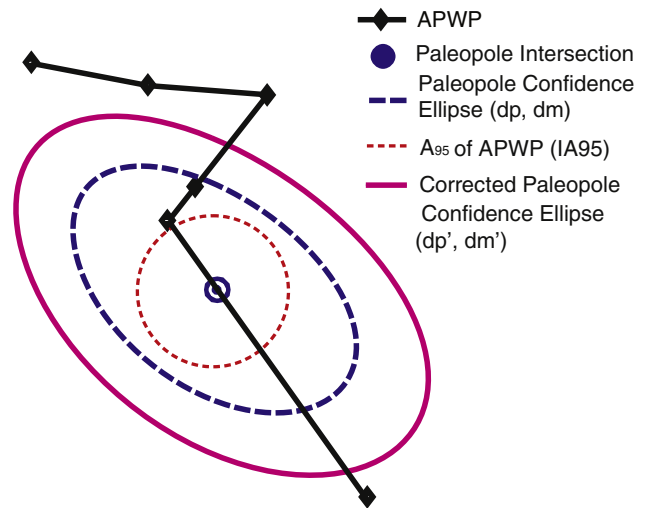


Fig. 6. Illustration of confidence ellipses of APWP (A_{95}), paleopole (α_{95}), and the corrected paleopole confidence ellipse (α_{95}').

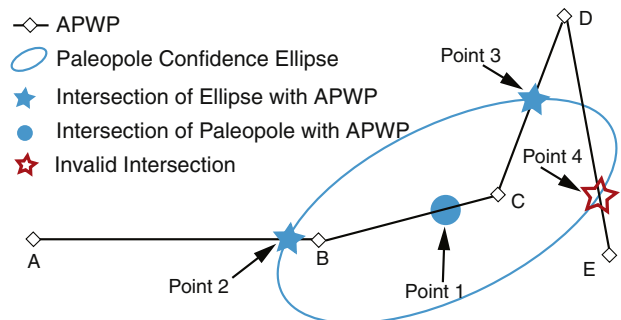


Fig. 7. Generalized diagram showing possible paleopole intersections with an APWP.

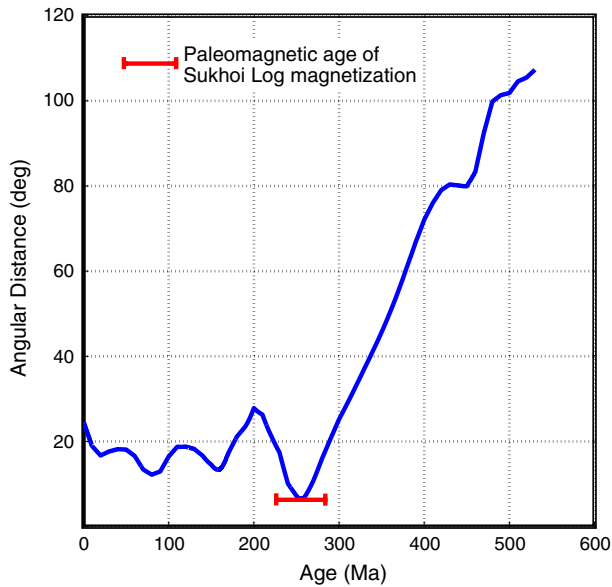


Fig. 8. Angular distance between the Sukhoi Log paleopole (this study) and the Siberian APWP (Torsvik et al., 2012). The most probable age occurs at the global minimum.

has an associated minimum angular distance to the APWP. Potential ages occur when minima occur in this dataset, with the global minimum(s) being considered the most likely (Fig. 9). In many cases the possible age(s) of the sample correspond to where the small circle intersects the APWP (i.e. angular distance is zero). Typically the amount of rotation is unknown so all intersections must be considered as possible ages unless ruled out by other means.

7. Using the paleomagnetic dating software

The paleomagnetic dating software used for this study currently requires Matlab. More detailed instructions and features are available from www.ualberta.ca/~vadim/software.htm. After executing the program a preliminary interface will load that allows a user to input the required parameters (e.g. site and paleopole location) and to load a reference curve from an excel worksheet (Fig. 10 top). This interface also provides stereographic projections that allow the plotting of paleomagnetic and geographic data. Once the user has inputted all the required information, clicking on the “Open Age Calculator” button will bring up a separate popup menu (Fig. 10 bottom). In this menu a pole, reference curve, and dating technique are selected. The user clicks on the “Calculate” button and the results are displayed in a data table, and the relevant plots are shown in the figure window. All data calculated (interpolated reference curves, ages, data locations, etc.) can be exported into an excel spreadsheet, and all figures can be saved into various image formats.

8. Discussion

8.1. Paleopole location and age

The APWP used for this study is the recommended Siberian APWP from the Torsvik et al.'s (2012) database. It is based on a spline model from Torsvik et al. (2012) that considers paleopoles from Siberia for ages of 250 Ma and older, and considers Laurasia paleopoles for ages younger than 250 Ma. The Torsvik et al.'s (2012) APWP is given in increments of 10 Ma and does not have associated A_{95} 's.

The Sukhoi Log paleopole (61.3°N, 155.9°E) calculated from the HTC in in-situ coordinates is situated near the late Palaeozoic and early Mesozoic portion of the Siberian APWP. The age of this paleopole was

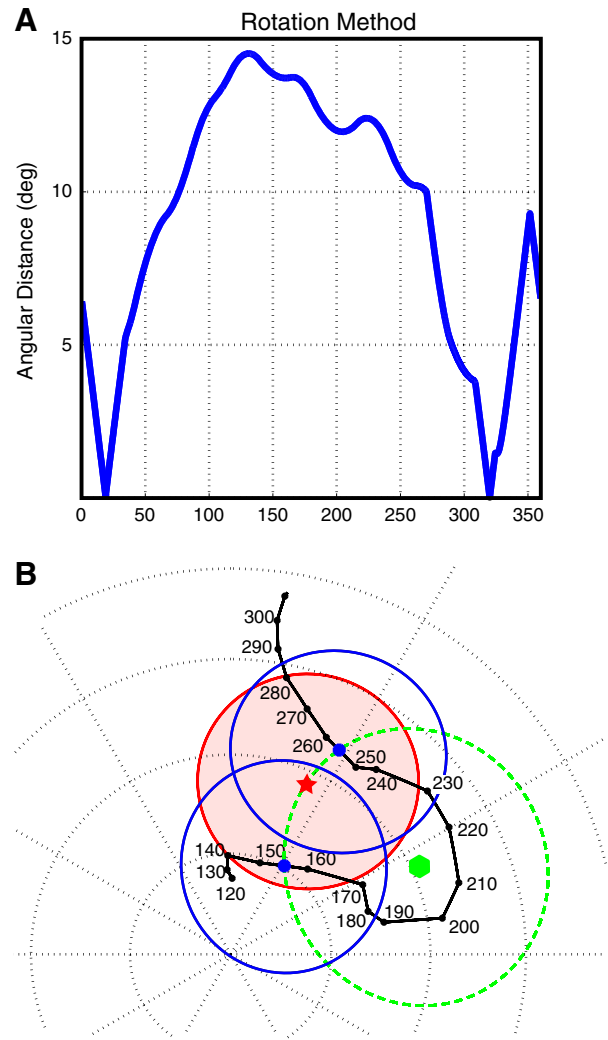


Fig. 9. A) Minimum angular distance between each point on the Sukhoi Log small circle (this study) and the Siberian APWP (Torsvik et al., 2012). The most probable ages occur when the angular distance is zero (i.e. an intersection). B) Stereographic projection of the Siberian APWP (Torsvik et al., 2012), Sukhoi Log paleopole (red star), small circle (green dashed line) of rotation around site location (green hexagon), and the rotated paleopoles (blue circle). APWP ages are given in millions of years.

determined using the paleomagnetic software developed for this study (Fig. 11). The angular method described above was chosen as the most appropriate method for Sukhoi Log because there is no large scale rotations documented at the site. All potential intersections were investigated provided that they met the criteria that they lay within the value of the paleopole's semi-major axis (16.6°). Three potential intersections were investigated. $80.0 \pm_{80.0}^{101.0}$ Ma, $158.3 \pm_{138.3}^{33.9}$ Ma, and $255.2 \pm_{31.0}^{32.0}$ Ma, based on translations of 12.20°, 13.36°, and 6.50° respectively. Out of the three contending ages the $255.2 \pm_{31.0}^{32.0}$ Ma is considered the most probable due to the intersection being nearly twice as close to that of the original paleopole compared to the younger ages (Fig. 8). The younger ages also do not have a defined lower bound intersections as only the upper bound intersection exists. This is due to all points of the APWP younger than the paleopole being enclosed within the paleopole's error ellipse.

8.2. Timing of major events at Sukhoi Log

The paleomagnetic data obtained in this study is the youngest well defined age associated with Sukhoi Log. The closest age reported in

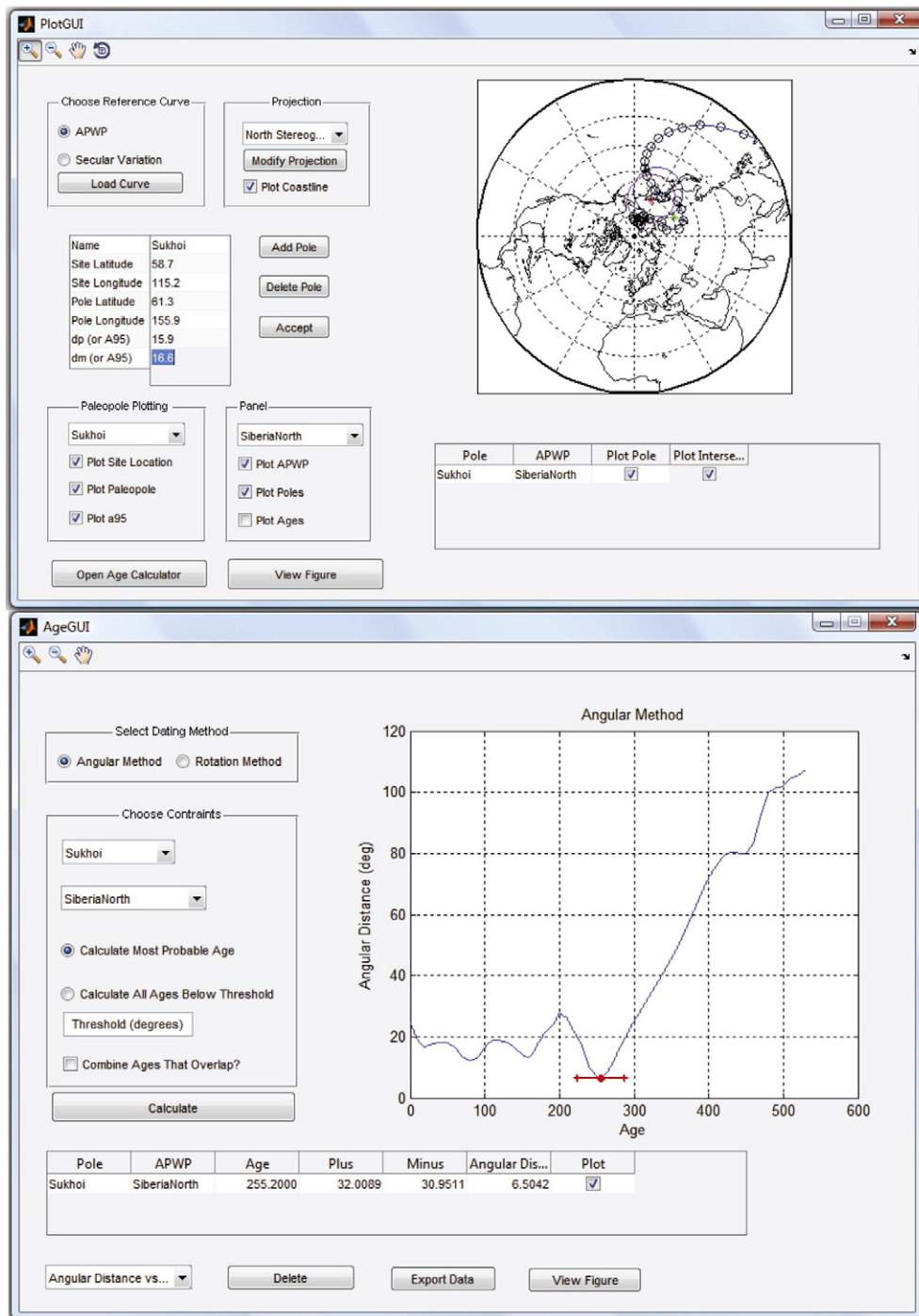


Fig. 10. Software interface.

previous studies is that of the 288 ± 22 Ma for monazite and the very broad Pb model ages for pyrite (200–400 Ma) from the Meffre et al.'s (2008) study. The monazite age in particular is nearly identical to that of the reported age (~290 Ma) of a small granite body located 6 km south-west of Sukhoi Log (Kuz'min et al., 2006). The age associated with the remanent magnetization ($255.2 \pm_{31.0}^{32.0}$ Ma) is somewhat younger than that of the monazite, but does overlap slightly, which suggests that they may be associated with the same event. Our paleomagnetic age verifies that large scale thermal or hydrothermal (or both) activity took place at Sukhoi Log during the late Paleozoic. Geologic activity must have persisted at Sukhoi Log until around ~250 Ma and is most likely related with the youngest stage of the Siberian Trap Province formation as suggested in Kuzmin et al. (2010). The granite body that

exists underneath the deposit is a possible candidate for imparting magnetization of this age as it is the only nearby body known that could provide the heat and/or fluid flow required to reset magnetization on the large scale required.

The paleomagnetic age does not determine whether the gold was introduced early on in Sukhoi Log's history (Large et al., 2007, 2009) or later through Palaeozoic technomagmatic activation (Distler et al., 2004; Laverov et al., 2007; Yudovskaya et al., 2011), but does provide timing of the last thermal or hydrothermal event that occurred at Sukhoi Log. The exact timeline of Sukhoi Log remains in flux as the early stages of the deposit are not well defined due to competing interpretations of metamorphism and host rock deposition ages (Distler et al., 2004; Meffre et al., 2008; Yudovskaya et al., 2011). Hydrothermal

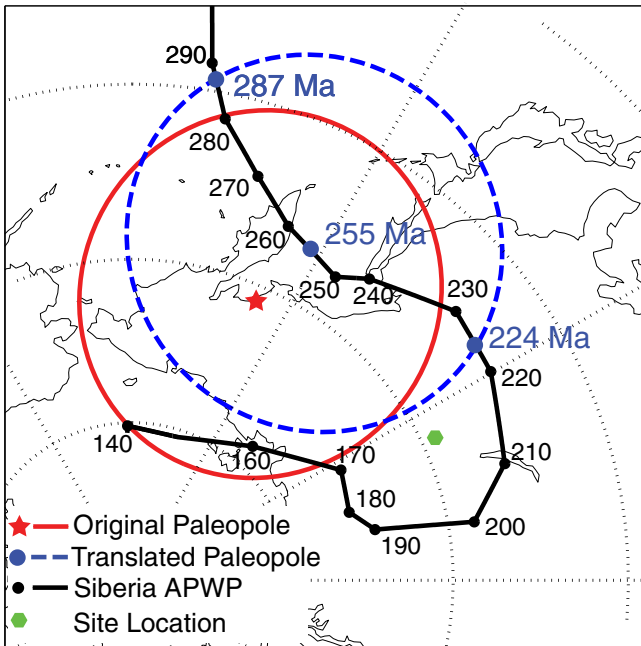


Fig. 11. Stereographic projection of the Siberian APWP (Torsvik et al., 2012), Sukhoi Log paleopole, and the expected translation of this paleopole onto the APWP.

events were likely common throughout Sukhoi Log's history with many potential events occurring between 250 and 500 Ma. Unfortunately, even with our new paleomagnetic data, this complex history continues to make it extremely difficult to pin down the exact details of gold mineralization and remobilization.

Based on previous studies and our paleomagnetic study we conclude that the majority of gold was imputed during diagenesis and early metamorphism based on the observations of Large et al. (2007, 2009). After the majority of the gold input was finished, many large scale events are known to have occurred, leading to the ages obtained by the monazite, Rb–Sr, and paleomagnetic studies. During these stages the gold was likely remobilized and other ore minerals (e.g. pyrite) formed to create the present day state of Sukhoi Log. Fig. 12 provides a summary of the known ages and events that are thought to have taken place at, or in the vicinity of, Sukhoi Log.

8.3. Reliability of paleomagnetic dating

The technique described in this study produces ages that are of the same order of magnitude as many isotopic dating techniques. This will allow paleomagnetic dates to meaningfully contribute to geochronologic studies. However, there are a few assumptions that were made in order to produce the paleomagnetic age in our study.

We have assumed that the only significant error for defining the age of the Sukhoi Log paleopole is that of the pole itself. Any uncertainty in the original Siberian APWP, and our subsequent interpolation, is considered insignificant. We have chosen the recommended path from Torsvik et al. (2012) which is a spline path that is smoothed to incorporate the quality of the input poles (Van der Voo, 1990, 1993). This Siberian APWP is well defined up to the Permian, but the lack of poles between the Permian and Silurian (in particular the Devonian) makes this APWP less robust for older Paleozoic ages. Our age (~250 Ma) is near the Permo-Triassic interval of the APWP, so any uncertainty in the older parts of the APWP is unlikely to greatly affect the age, and its resulting conclusions. The spline technique however assumes that the wander of the poles follows a smooth path through time. Our additional linear interpolation is not completely realistic, as poles typically move at variable rates between ~0.5 and 1° per million years (Torsvik et al., 2012), and any changes in the orientations of the continent will cause non-linear trajectories. However, without higher resolution data available we are required to make these assumptions to estimate where the APWP lies between the defined APWP poles. We expect that on these short timescales (<10 Ma) the deviation from these linear trajectories is insignificant in comparison to the paleopole error of ~16.5°.

Another major assumption with paleomagnetic dating is that we have properly interpreted the origin of the measured magnetization. Paleomagnetic ages do not discriminate between a primary age (age of the rock/mineral) and that of a remagnetization age. Remagnetization can occur in a number of ways, either by precipitating new magnetic minerals, or by resetting the magnetization of existing magnetic minerals. This is typically done by heating the rocks to several hundred degrees over an extended period of time or by introducing hydrothermal fluids into the system. Remagnetized samples therefore tend to record major episodes of thermal or hydrothermal disturbance of the sampled area (e.g. metamorphism). Due to these complexities paleomagnetic dating should be corroborated with supplemental geologic knowledge to pin down the exact nature of the magnetization. In our case the failed fold test indicates that we are not dealing with primary magnetization, but remanent magnetization.

Even with these assumption paleomagnetic dating is a useful tool for dating geologic objects. Due to its inherent ability to date essentially all rock types in a variety of geologic settings, paleomagnetic dating is particularly useful for areas with sparse or uncertain isotopic or biostratigraphic age constraints.

8.4. Further applications

The primary focus of this paper is to apply our newly developed software to date rocks using paleomagnetism. This software can also be used to supplement archeomagnetic studies using the same techniques described above. The only major difference between paleomagnetic and archeomagnetic dating is that the reference curves are defined differently. Our software at this time is not able to include paleointensity

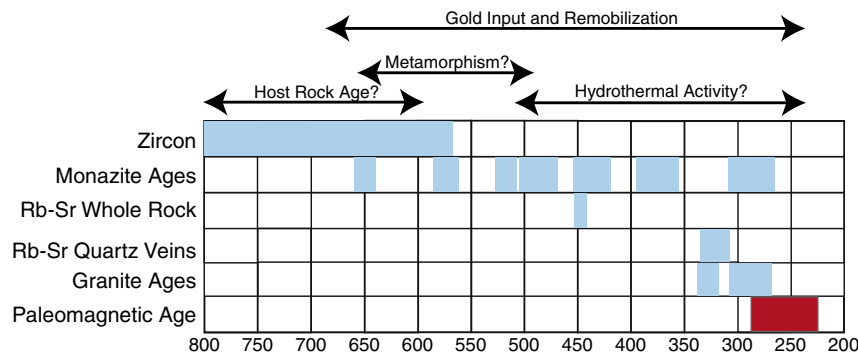


Fig. 12. Summary of the major events that have occurred at Sukhoi Log.

data for calculation as is used the Matlab program created by Pavon-Carrasco et al. (2011). However, paleointensity data is still relatively rare and our techniques can be used if a secular variation curve is loaded without paleointensity values. Another application of this software is for tectonic reconstruction studies. Often geologic terrains have undergone substantial rotations and therefore must be undone in order for paleopoles to be of use. Our software enables a user to rotate and plot rotated poles for use in tectonic or paleomagnetic dating studies. Finally, our program provides an easy to use interface to plot paleomagnetic or geographic data in a variety of ways on an assortment of possible projections.

Acknowledgments

The study was partially funded by the Natural Sciences and Engineering Research Council of Canada (NSERC) of V.K. The paper benefitted greatly from the comments and suggestions of J. Meert and an anonymous reviewer.

References

- Blanco, D., Kravchinsky, V.A., Konstantinov, K.M., Kabin, K., 2013. Paleomagnetic dating of Phanerozoic kimberlites in Siberia. *J. Appl. Geophys.* 88, 139–153.
- Cogné, J.-P., 2003. PaleoMac: A Macintosh™ application for treating paleomagnetic data and making plate reconstructions. *Geochem. Geophys. Geosyst.* 4 (1), 1007. <http://dx.doi.org/10.1029/2001GC000227>.
- Distler, V.V., Yudovskaya, M.A., Mitrofanov, G.L., Prokof'ev, V.Y., Lishnevskii, E.N., 2004. Geology, composition, and genesis of the Sukhoi Log noble metals deposit, Russia. *Ore Geol. Rev.* 24, 7–44.
- Enkin, R.J., 1996. A Computer Program Package for Analysis and Presentation of Paleomagnetic Data. Pacific Geoscience Centre, Geological Survey of Canada.
- Enkin, R.J., 2003. The direction–correction tilt test: an all-purpose tilt/fold test for paleomagnetic studies. *Earth Planet. Sci. Lett.* 212, 151–166.
- Fisher, R., 1953. Dispersion on a sphere. *Proc. R. Soc. London A* 217, 295–305.
- Hagstrum, J.T., Blinman, E., 2010. Archeomagnetic dating in western North America: an updated reference curve based on paleomagnetic and archeomagnetic data sets. *Geochem. Geophys. Geosyst.* 11 (6). <http://dx.doi.org/10.1029/2009GC002979>.
- Kirschvink, J.L., 1980. The least-squares line and plane and the analysis of paleomagnetic data. *Geophys. J. R. Astron. Soc.* 62, 699–718.
- Kravchinsky, V.A., Kabin, K., 2005. Apparent Polar Wander Path for Siberian Platform. American Geophysical Union, Fall Meeting abstract#GP11A-0007.
- Kravchinsky, V.A., Konstantinov, K.M., Courtillot, V., Valet, J.-P., Savrasov, J.I., Cherniy, S.D., Mishenin, S.G., Parasotka, B.S., 2002. Palaeomagnetism of East Siberian traps and kimberlites: two new poles and palaeogeographic reconstructions at about 360 and 250 Ma. *Geophys. J. Int.* 148, 1–33.
- Kravchinsky, V.A., Kabin, K., Konstantinov, K.M., Savrasov, J.I., 2004. Paleomagnetic dating of kimberlites: Siberian essay. American Geophysical Union, Spring Meeting, abstract GP31A-06.
- Kuzmin, M.I., Yarmolyuk, V.V., Kravchinsky, V.A., 2010. Phanerozoic hot spot traces and paleogeographic reconstructions of the Siberian continent based on interaction with the African large low shear velocity province. *Earth Sci. Rev.* 102, 29–59.
- Kuz'min, M.I., Yarmolyuk, V.V., Spiridonov, A.I., Nemerov, V.K., Ivanov, A.I., Mitrofanov, G.L., 2006. Geodynamic setting of gold ore deposits of the Neoproterozoic Bodaibo trough. *Dokl. Earth Sci.* 407, 397–400.
- Large, R.R., Maslennikov, V., Robert, F., Danyushevsky, L.V., Chang, Z., 2007. Multistage sedimentary and metamorphic origin of pyrite and gold in the giant Sukhoi Log deposit, Lena gold province, Russia. *Econ. Geol.* 102, 1232–1267.
- Large, R.R., Danyushevsky, L., Hollit, C., Maslennikov, V., Meffre, S., Gilbert, S., Bull, S., Scott, R., Emsbo, P., Thomas, H., Singh, B., Foster, J., 2009. Gold and trace element zonation in pyrite using a laser imaging technique: implication for the timing of gold in orogenic and Carlin-style sediment-hosted deposits. *Econ. Geol.* 104, 635–668.
- Larin, A.M., Rytsk, Y.Y., Sokolov, Y.M., 1997. Baikā–Patom Fold Belt. In: *Precambrian Ore Deposits of the East European and Siberian Cratons*. In: Rundqvist, D.V., Gillen, C. (Eds.), Elsevier, pp. 317–379.
- Laverov, N.P., Chernyshev, I.V., Chugayev, A.V., et al., 2007. Formation stages of the large scale noble metal mineralization in the Sukhoi Log deposit, East Siberia: results of Isotope Geochronological Study. *Dokl. Akad. Nauk* 415, 236–241 (*Doklady Earth Sciences (English Translation)*, v. 415, p. 810–814).
- Le Goff, M., Gallet, Y., Genevey, A., Warme, N., 2002. On archeomagnetic secular variation curves and archeomagnetic dating. *Phys. Earth Planet. Inter.* 134, 203–211.
- McFadden, P.L., 1990. A new fold test for paleomagnetic studies. *Geophys. J. Int.* 103, 163–169.
- McFadden, P.L., McElhinny, M.W., 1988. The combined analysis of remagnetization and direct observation in paleomagnetism. *Earth Planet. Sci. Lett.* 87, 161–172.
- Meffre, S., Large, R.R., Scott, R., Woodhead, J., Chang, Z., Gilbert, S.E., Danyushevsky, L.V., Maslennikov, V., Hergt, J., 2008. Age and pyrite Pb-isotopic composition of the giant Sukhoi Log sediment-hosted gold deposit, Russia. *Geochim. Cosmochim. Acta* 72, 2377–2391.
- Pavon-Carrasco, F.J., Rodriguez-Gonzalez, J., Osete, M.J., Torta, J.M., 2011. A Matlab tool for archaeomagnetic dating. *J. Archaeol. Sci.* 38, 408–419.
- Symons, D.T.A., Arne, D.F., 2005. Paleomagnetic constraints on Zn–Pb ore genesis of the Pillara Mine, Lennard Shelf, Western Australia. *Mineral. Deposita* 39, 944–959.
- Symons, D.T.A., Sangster, D.F., 1991. Late Devonian paleomagnetic age for the Polaris Mississippi Valley-type Zn–Pb deposit, Canadian Arctic Archipelago. *Can. J. Earth Sci.* 29, 15–25.
- Tanguy, J.C., Le Goff, M., Principe, C., Arrighi, S., Chillemi, V., LaDelfa, S., Patane, G., 2003. Archeomagnetic dating of Mediterranean volcanics of the last 2100 years: validity and limits. *Earth Planet. Sci. Lett.* 211, 111–124.
- Torsvik, T., Van der Voo, R., Preeden, U., Niocaill, C.M., Steinberger, B., Doubrovine, P.V., Hinsbergen, D.J.J., Domeier, M., Gaina, C., Tohver, E., Meert, J.G., McCausland, P.J.A., Robin, L., Cocks, M., 2012. Phanerozoic polar wander, palaeogeography and dynamics. *Earth-Sci. Rev.* 113, 325–368.
- Tsygankov, A.A., Matukov, D.I., Berezhnaya, N.G., 2007. Magma sources and stages of emplacement of the Late Paleozoic Granitoids in the West Transbaikalian Region. *Geol. Geofiz.* 48, 156–180.
- Van der Voo, R., 1990. Phanerozoic paleomagnetic poles from Europe and North America and comparisons with continental reconstructions. *Rev. Geophys.* 28, 167–206.
- Van der Voo, R., 1993. *Paleomagnetism of the Atlantic*. Cambridge University Press, Tethys and Iapetus Oceans p. 411.
- Wood, B.L., Popov, N.P., 2006. The giant Sukhoi Log gold deposit, Siberia. *Russ. Geol. Geophys.* 47, 317–341.
- Yudovskaya, M.A., Dister, V.V., Rodionov, N.V., Mokhov, A.V., Antonov, A.V., Sergeev, S.A., 2011. Relationship between metamorphism and ore formation at the Sukhoi Log gold deposit hosted in black slates from the data of U–Th–Pb isotopic SHRIMP-dating of accessory minerals. *Geol. Ore Deposits* 53, 27–57.
- Zhitkov, A.N., Kravchinsky, A.Ya., 1982. Paleomagnetic-metallogeny investigations of productive quartz–pyrite mineralization in the Lena Region (exemplified by “Glavnoe” deposit). In: Khrenov, P.M., Novosibirsk, SNIIGiMS (Eds.), *Geophysical Investigations of Deposits in the Eastern Siberia*, pp. 105–109 (in Russian).
- Zijderveld, J.D.A., 1967. A.C. demagnetization of rocks, analysis of results. In: Collinson, D.W., Creer, K.M., Runcorn, S.K. (Eds.), *Methods in Paleomagnetism*. Elsevier, Amsterdam, pp. 254–286.